Circular RNA Circ-0006302 Promotes the Growth, Migration, and Invasion of Cholangiocarcinoma Cells by Regulating the Mir-1299/PD-L1 Axis as a Competing Endogenous RNA

Weiqian Chen
Lishui Hospital of Zhejiang University
Liyun Zheng
Lishui Hospital of Zhejiang University
Songquan Wu
Lishui Hospital of Zhejiang University
Chenying Lu
Lishui Hospital of Zhejiang University
Bufu Tang
Lishui Hospital of Zhejiang University
Enqi Qiao
Lishui Hospital of Zhejiang University
Jingjing Song
Lishui Hospital of Zhejiang University
Shiji Fang
Lishui Hospital of Zhejiang University
Dan Wu
Lishui Hospital of Zhejiang University
Rongfang Qiu
Lishui Hospital of Zhejiang University
Chunmiao Chen
Lishui Hospital of Zhejiang University
Yang Gao
Lishui Hospital of Zhejiang University
Xiaoxi Fan
Lishui Hospital of Zhejiang University
Zhongwei Zhao
Lishui Hospital of Zhejiang University
Jiansong Ji (jijiansong@zju.edu.cn)
Zhejiang University https://orcid.org/0000-0001-6975-620X

Primary research

Keywords: circ-0006302, miR-1299, competing endogenous RNA, PD-L1, cholangiocarcinoma

Posted Date: June 23rd, 2021

DOI: https://doi.org/10.21203/rs.3.rs-638620/v1

Abstract

Background: Cholangiocarcinoma (CCA) is an aggressive malignancy with a poor prognosis, with no effective therapy other than surgical resection. Circular RNAs (circRNAs) serve as a brand-new class of transcription products among abundant cancer processes. Nevertheless, the mechanisms account for their modification in CCA remain unknown.

Methods: First, microarray sequencing was applied to detect the difference of circRNAs expression between CCA and corresponding non-tumor tissues. We utilized qRT-PCR to measure *circ-0006302* levels in CCA cells and specimens. Gain/loss of-function assays and animal model of CCA were performed for the purpose of revealing the functions of *circ-0006302* on the invasion, migration, and proliferation of CCA. We performed dual luciferase reporter, RNA-FISH and rescue assays for clarifying the mechanism behind.

Results: In CCA tissues and cell lines *circ-0006302* was highly expressed relatively. *In vitro*, overexpression of *circ-0006302* intensifies the epithelial-to-mesenchymal transition (EMT) and the invasion, migration, and growth of CCA cells; and intensifies the growth as well as metastasis of tumors in a CCA mouse model. Furthermore, it was elucidated that *circ-0006302* sponged miR-1299 to upregulate *PD-L1* expression. Through the process above, *circ-0006302* binds to miR-1299 and emancipates *PD-L1,* facilitating the invasion, migration, and proliferation in CCA cells. Momentously, the results obtained revealed that *circ-0006302* silencing elevated the expression of interferon (IFN)-γ, and interleukin (IL)-4 but diminished the IL-10 expression, while these effects could be reversed by miR-1299 inhibitor.

Conclusion: *circ-0006302* silence blocked the CCA progression via intensifying miR-1299-targeted downregulation of *PD-L1*. Our conclusion provides novel therapeutic tactics for treating this fatal disease.

Background

Cholangiocarcinoma (CCA), which can emerge at any position of the biliary tree, constitutes a heterogeneous group of malignancies, with traits of poor prognosis and high mortality[1, 2]. Surgical resection of CCA serves as a curative treatment, prolonging survival outcomes[3, 4]. Nonetheless, CCA has difficulty in the early diagnosis and clinical manifestation, which lead to a status that unresectable tumors at an advanced stage are presented in most patients[5]. The 5-year survival rate of patients who received hepatic resection is only 20–40%[6]. Unresectable cases of CCA show a median survival time of 6–12 months[7]. Besides, we remain to conform the efficacy of chemotherapy and radiotherapy in prolonging long-term survival[8, 9]. Consequently, new targets regulating CCA cells is necessary to be discovered.

Circular RNA (circRNA), one of non-coding RNA molecules without a 5 cap and a 3 poly (A) tail, constructs a circular configuration via covalent bonds[10, 11]. In many diseases including cancer, cardiovascular diseases, neurological disorders, circRNAs are identified to play an influential role. They have diverse functions, which includes protein scaffolds, microRNA (miRNA) sponges, and even translation templates[12–14]. Nevertheless, the study relevant to circRNAs and CCA is far from ample. In our study, it was identified that *circ-0006302* was relatively high expression in CCA tissues. We probed into the oncogenic effect of *circ-0006302* in CCA for the first time, which might contribute to the researches with a brand-new insight into the pathogenesis of this lethiferous disease.

PD-1, a receptor of the Ig superfamily which can interact with the specific ligands (PD-L), is capable of negatively regulating T cell antigen receptor signaling, consequently playing a role in maintaining self-tolerance[15]. For the purpose of escaping from the antitumor immune response, tumor cells alter the T cell activity, which contributes to the survival of tumor cells[16, 17]. It is worth noting that tumor cells can interact with CD8 + T cells and induce their apoptosis, thus promoting tumor growth and metastasis[18, 19]. Moreover, plenty of studies have offered convincing evidence that neutralizing PD-L1 or PD-1 to block the PD-1/PD-L1 was able to activate CD8 + T cells and attenuate the immune evasion of tumor cells, which indicates that antibody against PD-1 and PD-L1 may be a potential treatment for cancers[20, 21]. In CCA patients, *PD-L1* overexpression was reported, and the expression of *PD-L1* was a separate prognostic element of CCA patients[22, 23].

In this study, we found *circ-0006302* displayed high expression in CCA tissues. Also, we identified a new mechanism by which *circ-0006302* sponged miR-1299 to upregulate *PD-L1* expression, so that to intensify the migration, proliferation, and invasion of CCA.

Methods

Patients and clinical sample collection

From 2017 to 2019, we harvested CCA and paired non-tumor tissue samples from 60 patients without receiving chemotherapy or radiotherapy before the study. After retrieval we placed samples in liquid nitrogen instantly. We provided informed consent for the involved, and our research gained approval by the Ethics Committee of Lishui Hospital of Zhejiang University.

Cells and cell culture

We purchased human CCA cell lines (TFK-1, SNU-869, RBE, HuCCT1 and HuH28), normal human intrahepatic biliary cell (HIBEC), and HEK293T cells from the Chinese Academy of Scien ces (Shanghai, China). We maintained cells in a humidified atmosphere at 37 °C and 5% CO_2 in RPMI-1640 (Gibco, Grand Island, NY, USA), which contains 10% fetal bovine serum (Invitrogen Life Technologies, Carlsbad, CA, USA). We cultivated HEK293T cells in 10% FBS DMEM/high glucose medium. All cell lines were passaged for less than 6 months.

circRNAs Microarray and Data Analysis

With Arraystar Human circRNA Array V2 we analyzed three pairs of CCA and non-tumor tissue samples. With the NanoDrop ND-1000 we quantified total RNA from each sample. In conformity with the Arraystar's standard protocols we conducted the microarray hybridization and sample preparation. In brief, we digested total RNAs with Rnase R (Epicentre Technologies, Madison, WI, USA) for removing linear RNAs and enriching circular RNAs. Afterward, with a random priming method (Arraystar Super RNA Labeling Kit; Arraystar) we amplified the enriched circular RNAs and transcribed them into fluorescent cRNA. We hybridized the labeled cRNAs onto the Arraystar Human circRNA Array V2 (8x15K, Arraystar). With the Agilent Scanner G2505C we scanned the arrays after washing the slides. For analyzing obtained array images, we used Agilent Feature Extraction software (version 11.0.1.1). We performed subsequent data processing and quantile normalization with the R software

limma package. We performed hierarchical clustering for demonstrating the difference of circRNAs expression pattern in the midst of the samples.

Cell transfection

We purchased pLVX-EF1α, PLKO.1-puro and plasmid vectors from BioVector NTCC Inc., Guangzhou, China. A shRNA sequence that targeted *circ-0006302* and a negative shRNA control sequence were designed and synthesized, and we cloned them into PLKO.1-puro. The sequences which encode *circ-0006302*, *PD-L1*, and a negative control were also synthesized, and cloned into pLVX-EF1α. We purchased the miR-1299 mimics and miR-1299 inhibitor from RIBOBIO, Guangzhou, China. We cultured cells for 24 hours, and transfected them with plasmids via Lipofectamine 3000 Transfection Reagent (Invitrogen, Carlsbad, CA, USA), per manufacturer's instructions. We harvested cells to conduct RNA extraction after 48 hours. We performed the experiments in triplicate.

RNA extraction and Quantitative real-time polymerase chain reaction (qRT-PCR)

Centrifugation was performed at 4 °C. From the upper aqueous phase, we obtained the isopropanol precipitates at room temperature (20–25 °C), then based on the TRIzol total RNA manual (Invitrogen, Carlsbad, CA, USA) we rinsed and dried them. Consequently, DEPC-treated water was added and for each sample we calculated the RNA concentration. At -80 °C we stored the RNA. Via the OneStep PrimeScript® miRNA cDNA Synthesis Kit (Takara) we generated cDNA, per manufacturer's instructions. SYBR Green I fluorescence method was applied to conduct RT and we carried out PCR detection. We utilized primer sequences listed in Table 1. $2^{-\triangle\triangle Ct}$ for calculating the relative concentration of the samples. We performed the experiments in triplicate.

Table 1

Sequences of primers for qRT-PCR

Name	Sequence	
circ-0006302	Forward	5’- GCTGGGCAGGAAAACCTATT-3’
Reverse	5’-TTTCCCAGGTCTCTGTCTGG-3’	
E-cadherin	Forward	5’- GCTGGACCGAGAGAGTTTCC -3’
	Reverse	5’- CAAAATCCAAGCCCGTGGTG -3’
Vimentin	Forward	5'- CGGGAGAAATTGCAGGAGGA -3'
	Reverse	5'-AAGGTCAAGACGTGCCAGAG-3'
Snail	Forward	5'-TCGGAAGCCTAACTACAGCGA-3'
	Reverse	5'-AGATGAGCATTGGCAGCGAG-3'
miR-1299	Forward	5'-ACACTCCAGCTGGGAGGGAGUGUGUCUUAA-3'
	Reverse	5'-CTCAACTGGTGTCGTGGAGTCGGCAATTCAGTTGAGTTCTGGAT-3'
PD-L1	Forward	5'- GGTGAGGATGGTTCTACACAG -3'
Reverse	5'-GAGAACTGCATGAGGTTGC-3'	

RNase R digestion

3 units of RNase R (Epicentre Biotechnologies) per 1 μg *circ-0006302* were added and at 37 °C we incubated the mixture for 15 minutes. Consequently, qRT-PCR was performed to assess the levels of GAPDH and *circ-0006302*.

Western blotting

Total cell lysates were prepared in 1× sodium dodecyl sulfate (SDS) buffer. By polyacrylamide gel electrophoresis we separated protein lysates and transferred them onto nitrocellulose membranes. In 5% non-fat milk we blocked membranes, then incubated them with primary antibodies to PD-L1 (ab205921; 1: 1000), E-cadherin (ab40772; 1:10000), Snail (ab216347; 1: 1000), and vimentin (ab45939; 1: 1000) at 4 °C overnight. Afterward, we incubated them with goat anti-rabbit secondary antibody (Abcam, Shanghai, China). We performed the experiments in triplicate.

Cell counting kit-8 assay

We utilized cell Counting Kit-8 (Beyotime Inst Biotech, China) to assess cell proliferation. In brief, into 96-well plates we seeded 5×10^3 cells/well. The cells were transfected with appropriate plasmids and controls after 24 hours. To assess proliferation a microplate reader (Bio-Rad, Hercules, CA, USA) (absorbance wavelength 450 nm) was used. We performed the experiments in triplicate.

Colony formation assay

In 6-well plates we seeded cells and in media containing 10% FBS we cultured them. The cells were fixed with methanol after 14 days, and with 0.1% crystal violet (Sigma-Aldrich) we stained them, then we counted clones. We performed the experiments in triplicate.

Ethynyl-2-deoxyuridine (EdU) incorporation assay

Ethynyl-2-deoxyuridine incorporation assay (EdU Apollo DNA in vitro kit, RIBOBIO, Guangzhou, China) was utilized to identify cell proliferation, per manufacturer's instructions. In brief, we added 100 µl of 50 µM EdU/well after transfecting cells with plasmids, and incubated the cells at 37 °C for 2 hours. Fluorescence microscopy was used for determining proliferation. We performed the experiments in triplicate.

Wound healing and transwell invasion assays

We cultured the different groups of CCA cells (1×10^6 cells/well) up to 90% confluency and with a sterile pipette tip (100 µl) we scratched the monolayer of cells in individual wells. We cultured the cells continually for 24 h and imaged them at 0 and 24 h post scratching with a digital camera (Leica, Heerburg, Germany). By the distance of migration into the denuded area we assessed the extent of wound healing.

Transwell^{TM} chambers coated with Matrigel were utilized. We resuspended cells (5×10^4/L) in 200 µL serum-free medium and seeded them into the upper chambers. To the lower chambers 600 µL complete medium were added. We wiped cells that remained on the upper filter surface away after 48 hours at 37 °C. With formaldehyde we fixed cells migrated to the bottom of the filter and with crystal violet we stained them. Under an Olympus fluorescence microscope (Tokyo, Japan) we counted the cella.

RNA fluorescent in situ hybridization (FISH)

In short, we placed the cover glasses on the bottom of a 24-well plate, and cultured the cells with 6×10^4 cells per well. We waited until the cell confluence reached about 60%–70%, then we fixed them in 4% paraformaldehyde and with the precooled permeation reagent (1 ml/well) we permeabilized them. With the prehybridization solution (20 µl/well) we sealed the cells and hybridized them with the Stellaris RNA FISH solution (Biosearch Technologies, Petaluma, CA), which contains the probe for *circ-0006302*. Then we rinsed the cells by lotion I, lotion II, lotion III, and 1× PBS ultimately. Consequently, we stained the cells for 10 min with FAM fluorescent dye liquor. Finally, with a mounting agent (like nail polish) we fixed the cover glasses on the glass slides, and under a fluorescence microscope (Olympus) we viewed them for fluorescence detection.

Dual-luciferase reporter assays

We established and amplified *circ-0006302* wild type or *PD-L1* wild type, which contained mutant sequences with target sites deletion or designed miR-1299 binding sites before they were cloned into the pRL-TK plasmid (Promega) vector. After that, HEK293T cells were seeded (2×10^4 cells/well) into 96-well plates. We co-transfected the cells with the luciferase plasmids (0.1 μg/well) and miR-1299 mimics or controls. We assessed firefly and renilla luciferase activity using the Dual-Luciferase Reporter Assay System (Promega) after two days as mentioned above.

Tumor xenograft implantation in nude mice

From Beijing HFK Bioscience, Beijing, China we gained male BALB/c nude mice (4 weeks old). In compliance with the institutional guidelines of Lishui Hospital of Zhejiang University, we designed the protocol and in obedience to the Use Committee for Animal Care we implemented the animal studies. In serum-free medium we suspended the stable transfection of RBE cells (1×10^7 cells/ml) with *circ-0006302* or vector, and injected the cells in the right flank of the mice subcutaneously. After injection we assessed the tumors every 7 days. We calculated tumor volumes (as a rotational ellipsoid) with length × width^2 × 0.5. 4 weeks later we sacrificed the mice and tumors weights were recorded.

Immunohistochemistry

Stained with H&E, representative areas were evaluated. With antibodies to Ki-67 (ab15580) (Abcam, Shanghai, China) we performed immunohistochemistry per manufacturer's instructions.

Statistical analyses

We performed the paired Student's *t*-test for detecting the differential expression of *circ-0006302* and miR-1299 between CCA tissues and para-cancerous normal tissues. We then evaluated the deviations by one-way ANOVA or unpaired Student's t-test (other 2-group comparisons) before the post hoc Bonferroni test (multigroup comparisons) as appropriate. Via the Kaplan–Meier survival curves and log-rank test we analyzed the overall survival rates. Also, by Pearson’s correlation analysis we validated the relationships between *circ-0006302* and *PD-L1*. By Fisher’s exact test we analyzed the association between *circ-0006302* expression and clinicopathological characteristics of CCA patients. We displayed the data as the mean ± standard deviation; if $p < 0.05$ statistical significance was considered. All statistical tests were performed with SPSS version 19.0 software (SPSS Inc. Chicago, IL, USA).

Results

Circ-0006302 expression is up-regulated in CCA tissues and cell lines

Via microarray sequencing we detected the circRNAs expression in CCA tissues and corresponding non-tumor tissues, which were harvested from three CCA patients. After analyzing microarray results, we found *circ-0006302* showed high expression in the CCA tissues. Based on the criteria of log2 fold change > 2 or < -2 and P value < 0.05, we identified different expression of circRNAs. In the heatmap we showed the differentially expressed circRNAs including *circ-0006302* (Fig. 1A). Then, *circ-0006302* was verified by Sanger sequencing and RNase R treatment. The *circ-0006302* sequence amplified by the primer was confirmed to be identical to the sequence in Circbase, which was derived by Sanger sequencing (Fig. 1B). We then validated the circular structure of *circ-0006302*, which presented more stable resistant to RNase R (Fig. 1C). Compared with the corresponding non-tumor controls, *circ-0006302* expression was remarkably higher in tumor tissues (Fig. 1D). Expression of *circ-0006302* was remarkably higher in the CCA cell lines (TFK-1, RBE, SNU-869, HuH28 and HuCCT1) than in HIBEC, which was consistent with data above (Fig. 1E).

Circ-0006302 promotes the growth of CCA cells

Whether *circ-0006302* regulates the growth of CCA cells was then investigated. Initially, HuCCT1 cell line was co-cultured with sh-*circ-0006302*, and RBE cell line was co-cultured with *circ-0006302* overexpression vector, respectively (Fig. 2A). The proliferation of CCA cells curves was identified via CCK-8 assays, EdU assay, and colony-formation assays. Cell growth and colony-forming ability were inhibited in HuCCT1 cells by *circ-0006302* knockdown (Fig. 2B-D). The proliferation and colony-forming ability of RBE cells were intensified by *circ-0006302* overexpression (Fig. 2B-D). With these data we suggest that in vitro *circ-0006302* intensifies the growth of CCA cells.

Circ-0006302 stimulates cell migration, invasion, and the EMT of CCA cells

Whether *circ-0006302* impacted on the invasion and migration of CCA cells was evaluated. Wound healing assay showed that knockdown of *circ-0006302* inhibited the migration of HuCCT1 cells and overexpression of *circ-0006302* enhanced the migration of RBE cells (Fig. 3A). Via transwell invasion assays we observed a similar pattern of data in HuCCT1 and RBE cells (Fig. 3B).

Whether *circ-0006302* modulated the EMT of CCA cells was further investigated. Western blotting and qRT-PCR were utilized to assess the expression of involved mRNAs and proteins in the EMT. In HuCCT1 cells, *circ-0006302* knockout diminished vimentin and snail expression yet stimulated E-cadherin expression. While in RBE cells *circ-0006302* overexpression stimulated vimentin and snail expression yet diminished E-cadherin expression (Fig. 3C, D). With these results we suggested that in CCA cells *circ-0006302* intensifies cell invasion, migration, and the EMT.

Circ-0006302 promotes PD-L1 expression by binding to miR-1299

Potential molecular roles and biological function significantly affected by the subcellular localization of circRNAs. Initially, we utilized RNA-FISH to explore the subcellular localization of *circ-0006302*. It was showed

that majority of the positives located in the cytoplasm, while in the nucleus minority remained (Fig. 4A). Previous studies showed that *PD-L1* drives metastasis and initiation of CCA[24–26]. We performed qRT-PCR for investigating the mechanisms under *circ-0006302*-mediated biological processes. It was showed that there was a positive correlation between *circ-0006302* expression levels and *PD-L1* expression levels in CCA (Fig. 4B). Compared with HIBEC cell line, *PD-L1* was increased in CCA cell lines (Fig. 4C). Also, knockdown of *circ-0006302* decreased *PD-L1* expression in CCA cells (Fig. 4D). We speculated that *circ-0006302* may regulate *PD-L1* expression through competing endogenouse RNA mechanism. We then searched online bioinformatics database (TargetScan and CircInteractome) and performed bio-information analysis, which predicted that both miR-1299 and miR-876-3p have common putative binding sites with *circ-0006302* and *PD-L1* (Fig. 4E). Then, the level of two miRNAs were tested in CCA and HIBEC cell line, compared with HIBEC cell line only miR-1299 showed low expression level in CCA cell lines (Fig. 4F). As expected, compared with paired non-tumor tissue miR-1299 expression displayed remarkably lower levels in CCA tissues (Fig. 4G). Moreover, as bioinformatics analysis showed in Fig. 4H, the seed sequence of miR-1299 and the 3'UTR sequence of *PD-L1* was complementary. According to dual-luciferase reporter assay results, *circ-0006302*-Wt and miR-1299 mimics co-transfection remarkably attenuated luciferase activity, while *circ-0006302*-Mut and miR-1299 mimics co-transfection couldn't affect luciferase activity. Moreover, the similar results were observed in the luciferase activity of cells transfected with *PD-L1*-Wt (Fig. 4H). Whether *circ-0006302* modulated the expression of *PD-L1* via miR-1299-dependent manner in CCA cells was further determined. Results showed that miR-1299 overexpression diminished *PD-L1* expression in CCA cells (Fig. 4I). Besides, the *PD-L1* expression inhibition induced by silencing *circ-0006302* in CCA cells could be reversed by miR-1299 knockdown (Fig. 4J). Overexpression of miR-1299 reversed the increase in *PD-L1* expression of CCA cells induced by up-regulated of *circ-0006302* (Fig. 4K). The results indicated that in CCA cells *circ-0006302* positively regulates *PD-L1* expression through sponging miR-1299.

Circ-0006302 knockdown reverses the PD-L1 overexpression-induced increase in proliferation and invasion of CCA cells.

Hence, we explored if *circ-0006302* impacted on the invasion and proliferation of CCA cells via a *PD-L1*-dependent mechanism. HuCCT1 cells co-transfected with *PD-L1* overexpression vectors (with or without sh-*circ-0006302*). QRT-PCR and western blotting assays showed that *PD-L1* overexpression vectors significantly increased the RNA and protein level of *PD-L1*, while, the increase of *PD-L1* can be partially reversed by co-transfection with sh-*circ-0006302* (Fig. 5A). Besides, it was found that *circ-0006302* silencing remarkably reversed the improvement of growth and colony-forming ability induced by *PD-L1* overexpression in HuCCT1 cells (Fig. 5B, C). Similarly, *circ-0006302* silencing significantly reversed the improvement of invasive ability induced by *PD-L1* overexpression in HuCCT1 cells (Fig. 5D). Therefore, we indicate that in a *PD-L1*-dependent manner *circ-0006302* impacts on the invasion, migration, and growth of CCA cells.

Overexpression of circ-0006302 promotes the growth and metastasis of tumors in a mouse model of CCA

It was found that upregulation of *circ-0006302* promoted tumor growth in a CCA mouse model (Fig. 6A-C). In Fig. 6A we displayed tumors dissected from the mice. The tumors in the *circ-0006302* group were bigger (Fig. 6B) and heavier (Fig. 6C) compared with the vector treatment group. Besides, the expression of Ki-67 was lower in

vector group than in *circ-0006302* group (Fig. 6D). In Fig. 6E pulmonary metastasis slices are showed. With these results we indicate *circ-0006302* intensifies the growth and metastasis of CCA tumors in vivo.

Circ-0006302 competitively binds to miR-1299 to up-regulate PD-L1, thereby inhibiting the activation of CD8 + T cells

The sh-NC, sh-*circ-0006302*, vector, *circ-0006302* overexpression vector (*circ-0006302*), inhibitor NC (inh-NC), and miR-1299 inhibitor (miR-1299 inh) were delivered into the HuCCT1 cells respectively, then HuCCT1 cells and CD8 + T cells were cocultured. We utilized ELISA to determine the levels of antitumor cytokines IFN-γ and IL-4 as well as pro-tumor cytokine IL-10 (Fig. 7A). We found that after the delivery of sh-NC, inh-NC, vector or miR-1299 inh + sh-*circ-0006302* significant changes didn't emerge in the levels of IFN-γ, IL-10, and IL-4 in the cocultured CD8 + T and HUCCT1 cells. However, sh-*circ-0006302* transfection exhibited a decreased level of IL-10 yet increased levels of IL-4 and IFN-γ, whereas *circ-0006302* transfection led to a higher IL-10 level yet lower levels of IL-4 and IFN-γ. Via flow cytometry we identified no obvious change emerged in the apoptosis of CD8 + T cells transfected with inh-NC, vector, sh-NC or miR-1299 inh + sh-*circ-0006302*, however, the apoptosis of CD8 + T cells was notablely inhibited by transfection of sh-*circ-0006302* whereas intensified by *circ-0006302* overexpression (Fig. 7B). After the transfection of inh-NC, vector, sh-NC or miR-1299 inh + sh-*circ-0006302*, there is no noticeable change in the expression of *PD-L1* and PD-1. Nonetheless, the transfection of sh-*circ-0006302* could significantly reduce the expression of PD-1 and *PD-L1* yet *circ-0006302* overexpression could markedly increase the expression of PD-1 and *PD-L1*(Fig. 7C). In a whole, *circ-0006302* sponges miR-1299 and upregulates the expression of *PD-L1* to suppresse CD8 + T cell activation.

Discussion

Recently, circRNAs have emerged as crucial factors and influential regulators of gene expression in multiple cancers[27]. For example, circHIPK3 acts as a tumor-suppressive function in ovarian cancer[28]. Via activating JAK2/STAT3 signaling pathway, hepatocellular carcinoma progression was driven by circSOD2 induced epigenetic alteration[29] Circ-0000284 modulates the biological functions of peripheral cells via cellular communication and arouses malignant phenotype of CCA cells[30]. In this study, we observed *circ-0006302* expression levels in CCA tissues are distinctly higher than that in non-tumorous tissues. *Circ-0006302* knockdown attenuated the growth, invasion, and migration of CCA cells. In CCA, a positive correlation between the expression of *circ-0006302* and *PD-L1* was identified, and *circ-0006302* knockdown resulted in a synchronous drop in *PD-L1* expression. Besides, both *PD-L1* and *circ-0006302* were found to have the same putative binding sites in their 3'-UTRs, which was for the seed sequence of miR-1299.

The reduced expression and tumor-suppressive role of miR-1299 have been found in prostate cancer[31], ovarian cancer[32] and gastric cancer[33]. Meanwhile, through EGFR/PI3K/AKT signaling pathway, miR-1299 impedes the progression of NSCLC[34]. What's more, Xu and his colleagues found that miR-1299 serves as a tumor suppressor, thus inhibiting the metastasis and proliferation of CCA[35]. In this study, result of RNA-FISH exhibited that *circ-0006302* was mainly localized in the cytoplasm. QRT-PCR showed the expression of miR-1299 in CCA was lower level than in non-cancerous tissue. Also, miR-1299 overexpression decreased the expression of *PD-L1* and could significantly reversed the increase of *PD-L1* induced by overexpression of *circ-0006302*. Thus, *circ-0006302* may act as a ceRNA of miR-1299, to regulate *PD-L1.*

In subsequent experiments, *circ-0006302* silencing partly rescued the promotion of proliferation, migration, and invasion of CCA cells induced by upregulation of *PD-L1*. Importantly, we also determined that *circ-0006302* could suppress CD8 + T cell activation by sponging miR-1299 and upregulating the *PD-L1* expression subsequently.

Conclusion

In summary, we drew a conclusion that *circ-0006302* sequester miR-1299 by acting as a miRNA sponge. *Circ-0006302* binds with miR-1299, thus recruiting more *PD-L1* to participate in other interactions that promote the migration, growth, and invasion of CCA cells. In addition, *circ-0006302* upregulates the expression of *PD-L1* through sponging miR-1299 to suppress the cell activation of CD8 + T, thus helping CCA cells escape from the antitumor immune response (Fig. 8). Hence, our findings provide a new base for studying how CCA develops and progresses. Besides, our conclusion manifests that *circ-0006302* is a promising biomarker for CCA diagnosis and a potential target for its therapeutics.

Declarations

Ethics approval and consent to participate

Not applicable.

Consent for publication

Not applicable.

Availability of data and materials

The datasets used and/or analysed during the current study are available from the corresponding author on reasonable request.

Competing interests

The authors declare that the research was conducted in the absence of any commercial or financial relationships that could be construed as a potential conflict of interest.

Funding

This study was supported by the National Key Research and Development projects intergovernmental cooperation in science and technology of China [grant No. 2018YFE0126900], the National Natural Science Foundation of China [grant No. 82072025 and No. 82072026], the Cooperation Project of Zhejiang University and Lishui City [grant No. 2018zdhz06], the Science and Technology Project of Lishui City [grant No. 2019GYX27 and No. 2019SJZC61].

Authors' contributions

Jiansong Ji and Zhongwei Zhao designed the research and revised the manuscript; Weiqian Chen, Liyun Zheng and Songquan Wu performed the experiments; Chenying Lu, Bufu Tang, Enqi Qiao and Jingjing Song collected the data; Shiji Fang, Dan Wu and Rongfang Qiu did the analysis; Chunmiao Chen, Yang Gao and Xiaoxi Fan contributed to the Administration, technique and materials; Jiansong Ji drafted the manuscript; All authors approved the final manuscript.

Acknowledgements

Not applicable.

References

1. Kendall T, Verheij J, Gaudio E, Evert M, Guido M, Goeppert B, Carpino G. Anatomical, histomorphological and molecular classification of cholangiocarcinoma. Liver Int. 2019;39(Suppl 1):7–18.
2. Yu A, Zhao L, Kang Q, Li J, Chen K, Fu H. Transcription factor HIF1alpha promotes proliferation, migration, and invasion of cholangiocarcinoma via long noncoding RNA H19/microRNA-612/Bcl-2 axis. Transl Res. 2020;224:26–39.
3. Cillo U, Fondevila C, Donadon M, Gringeri E, Mocchegiani F, Schlitt HJ, Ijzermans JNM, Vivarelli M, Zieniewicz K, Olde Damink SWM, et al. Surgery for cholangiocarcinoma. Liver Int. 2019;39(Suppl 1):143–55.
4. Mahipal A, Kommalapati A, Tella SH, Lim A, Kim R. Novel targeted treatment options for advanced cholangiocarcinoma. Expert Opin Investig Drugs. 2018;27(9):709–20.
5. Mahipal A, Tella SH, Kommalapati A, Anaya D, Kim R. FGFR2 genomic aberrations: Achilles heel in the management of advanced cholangiocarcinoma. Cancer Treat Rev. 2019;78:1–7.
6. Jutric Z, Johnston WC, Hoen HM, Newell PH, Cassera MA, Hammill CW, Wolf RF, Hansen PD. Impact of lymph node status in patients with intrahepatic cholangiocarcinoma treated by major hepatectomy: a review of the National Cancer Database. HPB (Oxford). 2016;18(1):79–87.
7. Wasenang W, Chaiyarit P, Proungvitaya S, Limpaiboon T. Serum cell-free DNA methylation of OPCML and HOXD9 as a biomarker that may aid in differential diagnosis between cholangiocarcinoma and other biliary diseases. Clin Epigenetics. 2019;11(1):39.
8. Colyn L, Barcena-Varela M, Alvarez-Sola G, Latasa MU, Uriarte I, Santamaria E, Herranz JM, Santos-Laso A, Arechederra M, Ruiz de Gauna M, et al: **Dual targeting of G9a and DNMT1 for the treatment of experimental cholangiocarcinoma**. *Hepatology* 2020.
9. Rizzo A, Ricci AD, Bonucci C, Tober N, Palloni A, Frega G, Brandi G. **Experimental HER2 targeted therapies for biliary tract cancer**. *Expert Opin Investig Drugs* 2020.
10. Cai H, Li Y, Niringiyumukiza JD, Su P, Xiang W. Circular RNA involvement in aging: An emerging player with great potential. Mech Ageing Dev. 2019;178:16–24.
11. Ebbesen KK, Hansen TB, Kjems J. Insights into circular RNA biology. RNA Biol. 2017;14(8):1035–45.
12. Zeng Z, Xia L, Fan S, Zheng J, Qin J, Fan X, Liu Y, Tao J, Liu Y, Li K, et al: **Circular RNA CircMAP3K5 Acts as a MicroRNA-22-3p Sponge to Promote Resolution of Intimal Hyperplasia via TET2-Mediated SMC**

Differentiation. *Circulation* 2020.

13. Zhan W, Liao X, Chen Z, Li L, Tian T, Yu L, Wang W, Hu Q. **Circular RNA hsa_circRNA_103809 promoted hepatocellular carcinoma development by regulating miR-377-3p/FGFR1/ERK axis**. *J Cell Physiol* 2019.
14. Li HM, Ma XL, Li HG. Intriguing circles: Conflicts and controversies in circular RNA research. Wiley Interdiscip Rev RNA. 2019;10(5):e1538.
15. Iwai Y, Ishida M, Tanaka Y, Okazaki T, Honjo T, Minato N. Involvement of PD-L1 on tumor cells in the escape from host immune system and tumor immunotherapy by PD-L1 blockade. Proc Natl Acad Sci U S A. 2002;99(19):12293–7.
16. Nallasamy P, Chava S, Verma SS, Mishra S, Gorantla S, Coulter DW, Byrareddy SN, Batra SK, Gupta SC, Challagundla KB. PD-L1, inflammation, non-coding RNAs, and neuroblastoma: Immuno-oncology perspective. Semin Cancer Biol. 2018;52(Pt 2):53–65.
17. Del Re M, van Schaik RHN, Fogli S, Mathijssen RHJ, Cucchiara F, Capuano A, Scavone C, Jenster GW, Danesi R. Blood-based PD-L1 analysis in tumor-derived extracellular vesicles: Applications for optimal use of anti-PD-1/PD-L1 axis inhibitors. Biochim Biophys Acta Rev Cancer. 2020;1875(1):188463.
18. Zhang S, Zhong M, Wang C, Xu Y, Gao WQ, Zhang Y. CCL5-deficiency enhances intratumoral infiltration of CD8(+) T cells in colorectal cancer. Cell Death Dis. 2018;9(7):766.
19. Yan J, Allen S, McDonald E, Das I, Mak JYW, Liu L, Fairlie DP, Meehan BS, Chen Z, Corbett AJ, et al. MAIT Cells Promote Tumor Initiation, Growth, and Metastases via Tumor MR1. Cancer Discov. 2020;10(1):124–41.
20. Wang X, Guo G, Guan H, Yu Y, Lu J, Yu J. Challenges and potential of PD-1/PD-L1 checkpoint blockade immunotherapy for glioblastoma. J Exp Clin Cancer Res. 2019;38(1):87.
21. Yang J, Hu L. Immunomodulators targeting the PD-1/PD-L1 protein-protein interaction: From antibodies to small molecules. Med Res Rev. 2019;39(1):265–301.
22. Gani F, Nagarajan N, Kim Y, Zhu Q, Luan L, Bhaijjee F, Anders RA, Pawlik TM. Program Death 1 Immune Checkpoint and Tumor Microenvironment: Implications for Patients With Intrahepatic Cholangiocarcinoma. Ann Surg Oncol. 2016;23(8):2610–7.
23. Ma K, Wei X, Dong D, Wu Y, Geng Q, Li E. PD-L1 and PD-1 expression correlate with prognosis in extrahepatic cholangiocarcinoma. Oncol Lett. 2017;14(1):250–6.
24. Ganaie AA, Beigh FH, Astone M, Ferrari MG, Maqbool R, Umbreen S, Parray AS, Siddique HR, Hussain T, Murugan P, et al. BMI1 Drives Metastasis of Prostate Cancer in Caucasian and African-American Men and Is A Potential Therapeutic Target: Hypothesis Tested in Race-specific Models. Clin Cancer Res. 2018;24(24):6421–32.
25. Yoo YA, Roh M, Naseem AF, Lysy B, Desouki MM, Unno K, Abdulkadir SA. Bmi1 marks distinct castration-resistant luminal progenitor cells competent for prostate regeneration and tumour initiation. Nat Commun. 2016;7:12943.
26. Zhu S, Zhao D, Yan L, Jiang W, Kim JS, Gu B, Liu Q, Wang R, Xia B, Zhao JC, et al. BMI1 regulates androgen receptor in prostate cancer independently of the polycomb repressive complex 1. Nat Commun. 2018;9(1):500.
27. Chen B, Huang S. Circular RNA: An emerging non-coding RNA as a regulator and biomarker in cancer. Cancer Lett. 2018;418:41–50.

28. Teng F, Xu J, Zhang M, Liu S, Gu Y, Zhang M, Wang X, Ni J, Qian B, Shen R, et al. Comprehensive circular RNA expression profiles and the tumor-suppressive function of circHIPK3 in ovarian cancer. Int J Biochem Cell Biol. 2019;112:8–17.
29. Zhao Z, Song J, Tang B, Fang S, Zhang D, Zheng L, Wu F, Gao Y, Chen C, Hu X, et al. CircSOD2 induced epigenetic alteration drives hepatocellular carcinoma progression through activating JAK2/STAT3 signaling pathway. J Exp Clin Cancer Res. 2020;39(1):259.
30. Wang S, Hu Y, Lv X, Li B, Gu D, Li Y, Sun Y, Su Y. Circ-0000284 arouses malignant phenotype of cholangiocarcinoma cells and regulates the biological functions of peripheral cells through cellular communication. Clin Sci (Lond). 2019;133(18):1935–53.
31. Zhang FB, Du Y, Tian Y, Ji ZG, Yang PQ. MiR-1299 functions as a tumor suppressor to inhibit the proliferation and metastasis of prostate cancer by targeting NEK2. Eur Rev Med Pharmacol Sci. 2019;23(2):530–8.
32. Zhao L, Liu T, Zhang X, Zuo D, Liu C. lncRNA RHPN1-AS1 Promotes Ovarian Cancer Growth and Invasiveness Through Inhibiting miR-1299. Onco Targets Ther. 2020;13:5337–44.
33. Ding L, Wang L, Li Z, Jiang X, Xu Y, Han N. The positive feedback loop of RHPN1-AS1/miR-1299/ETS1 accelerates the deterioration of gastric cancer. Biomed Pharmacother. 2020;124:109848.
34. Cao S, Li L, Li J, Zhao H. MiR-1299 Impedes the Progression of Non-Small-Cell Lung Cancer Through EGFR/PI3K/AKT Signaling Pathway. Onco Targets Ther. 2020;13:7493–502.
35. Xu Y, Yao Y, Liu Y, Wang Z, Hu Z, Su Z, Li C, Wang H, Jiang X, Kang P, et al. Elevation of circular RNA circ_0005230 facilitates cell growth and metastasis via sponging miR-1238 and miR-1299 in cholangiocarcinoma. Aging. 2019;11(7):1907–17.

Figures

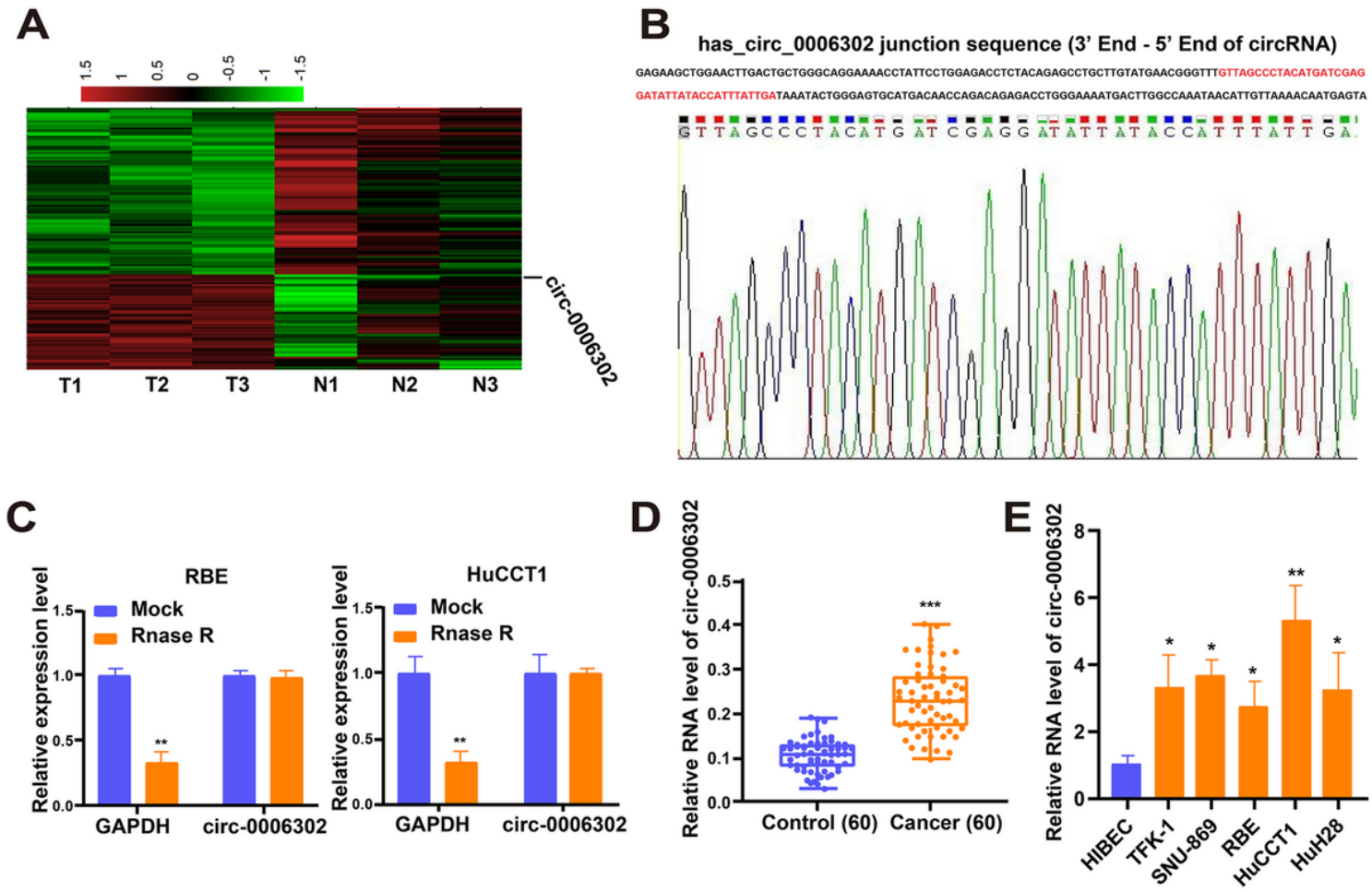

Figure 1

Relative circ-0006302 expression levels in CCA. (A) Heatmap of differentially expressed circRNAs including circ-0006302 in CCA tissue and paired non-tumor tissue counterparts. (B) Sanger sequencing. (C) RNase R digestion. (D) Circ-0006302 is elevated in CCA tissues. (E) Relative expression of circ-0006302 in CCA cell lines compared to that in HIBEC cells by qRT-PCR. *p < 0.05; **p < 0.01; ***p < 0.001.

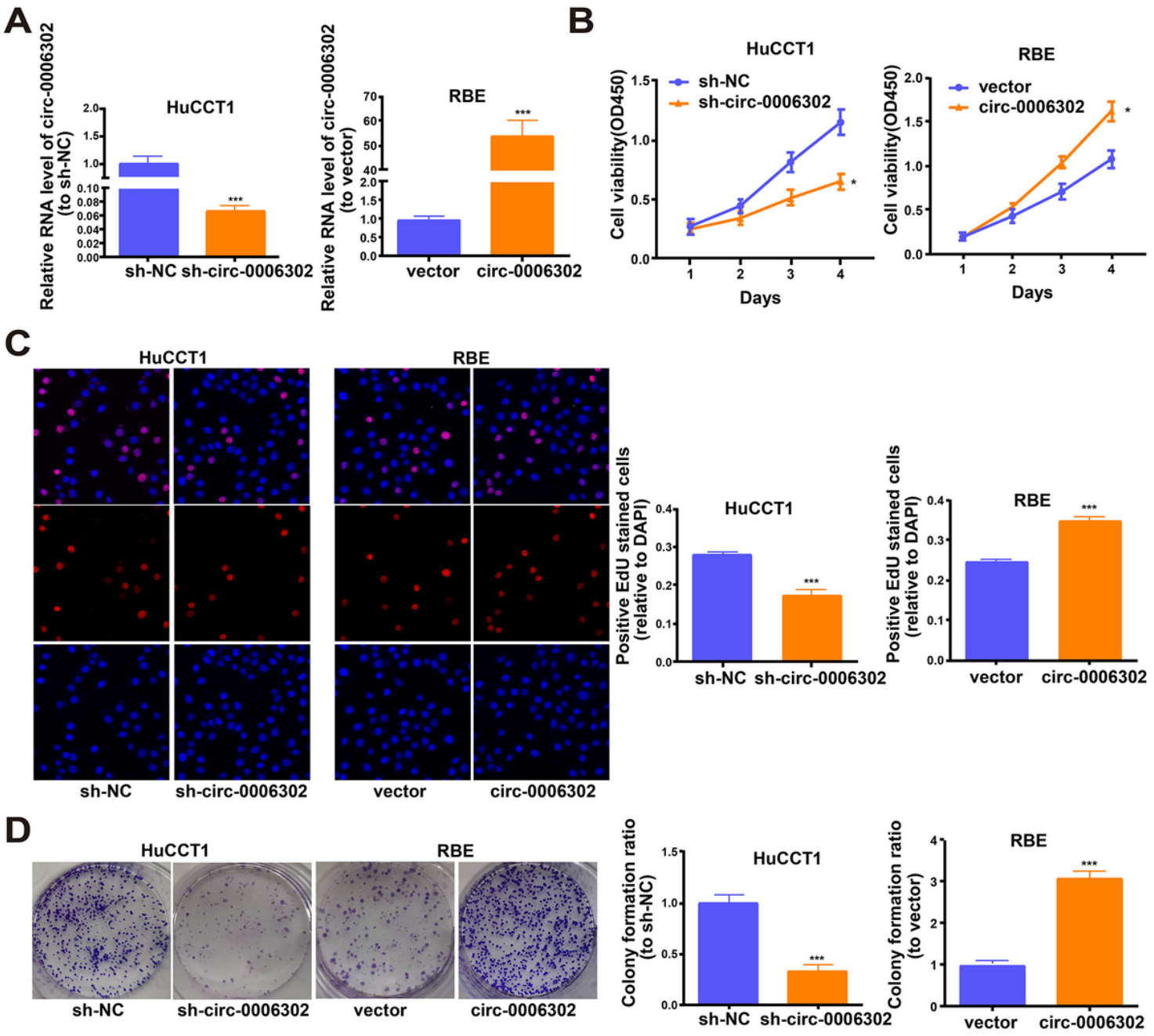

Figure 2

Circ-0006302 promotes the growth of CCA cells. (A) Transfection effectiveness of circ-0006302 shRNAs and circ-0006302 overexpression vector. (B-D) Proliferation of CCA cells by CCK-8 assay and colony-formation assay. Data represent the mean ± SD of 3 independent experiments; *p < 0.05; ***p < 0.001.

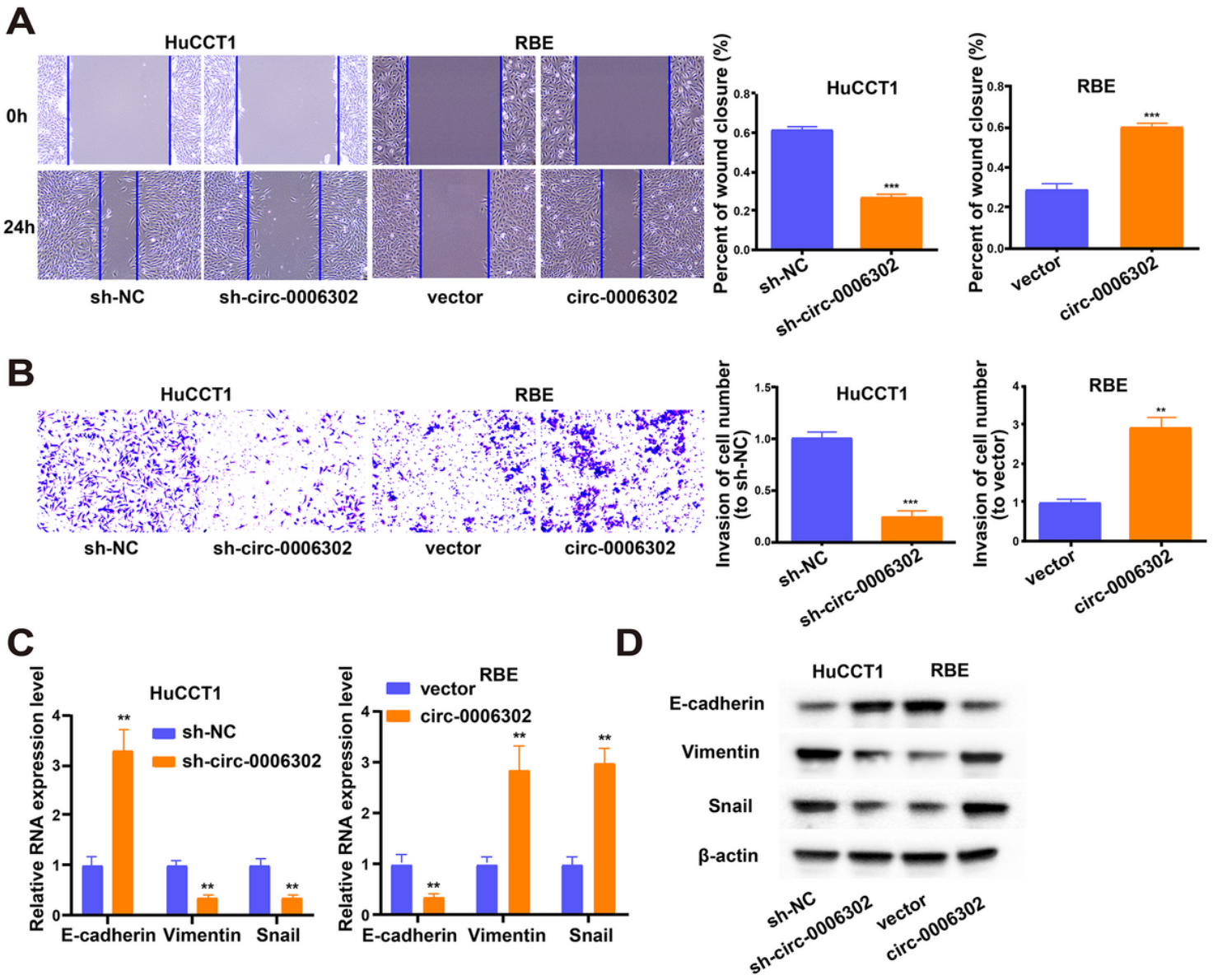

Figure 3

Circ-0006302 promotes the migration, invasion, and EMT of CCA cells. (A) The effect of circ-0006302 on the migration of CCA cells. (B) The effect of circ-0006302 on the invasion of CCA cells by transwell assay. (C, D) The effect of circ-0006302 on the expression of EMT indicators in CCA cells by qRT-PCR and western blotting. Data represent the mean ± SD of 3 independent experiments; **p < 0.01; ***p < 0.001.

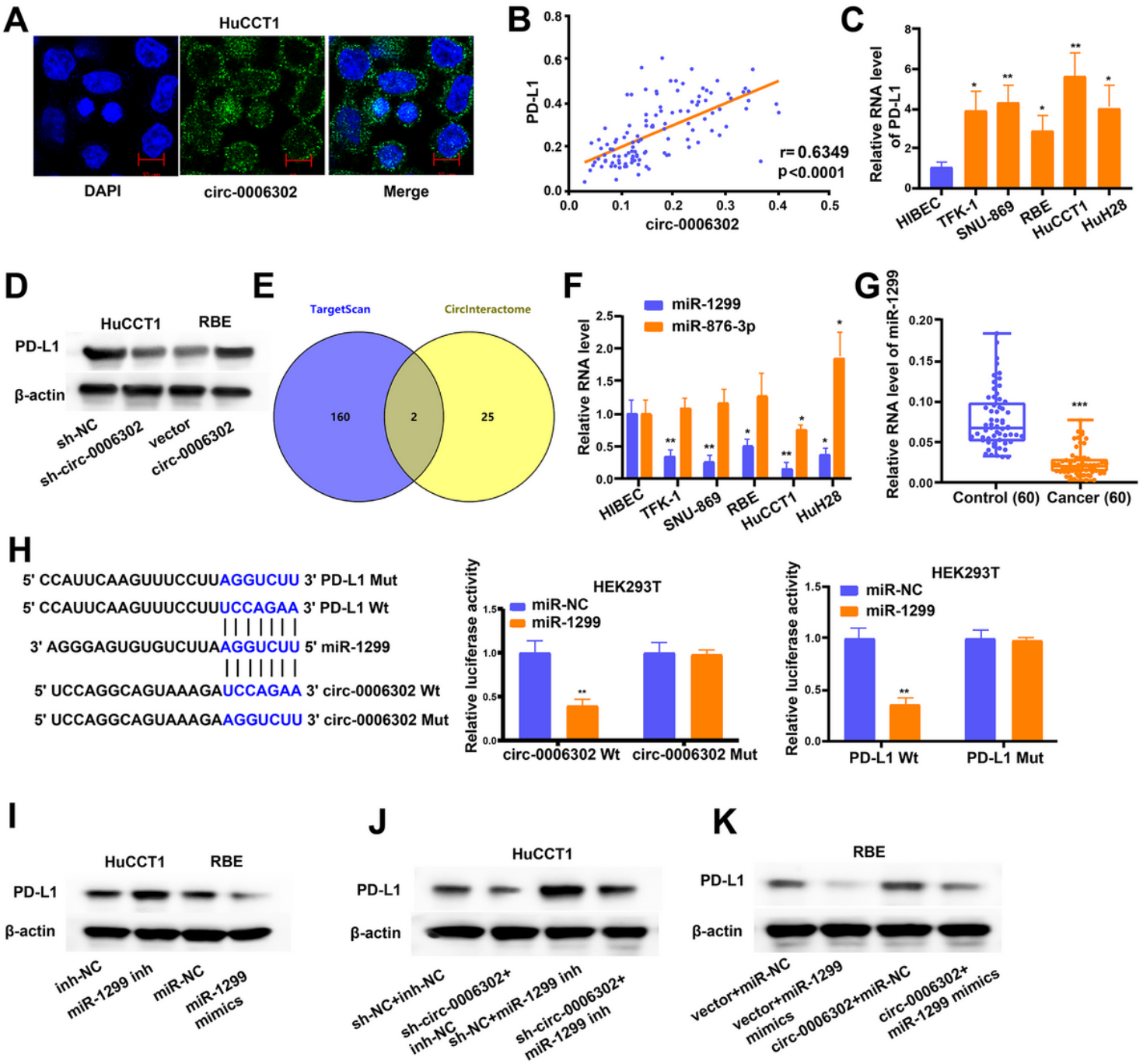

Figure 4

Circ-0006302 enhances PD-L1 expression by binding to the 3'-UTR of miR-1299. (A) Representative images of the subcellular localization of circ-001068 by RNA-FISH in CCA cells. (B) Evaluating the correlation of circ-0006302 and PD-L1 expression in CCA patient tissues by Pearson's correlation coefficient. (C) The level of PD-L1 in CCA cells. (D) The effect of circ-0006302 knockdown or overexpression on the expression of PD-L1 in CCA cells by western blotting. (E) Bioinformatics analysis with TargetScan and CircInteractome. (F) The levels of miR-1299 and miR-876-3p in CCA cell lines. (G) The level of miR-1299 in CCA tissues. (H) Dual-luciferase reporter assay and the binding sites. (I) The effect of miR-1299 on the expression of PD-L1 in CCA cells by western blotting. (J) The effect of miR-1299 inhibitor and shRNA-circ-0006302 on the expression of PD-L1 in CCA cells by western

blotting. (K) Overexpressing miR-1299 could reversed the increase of PD-L1 expression induced by circ-0006302 overexpression. Data represent the mean ± SD of 3 independent experiments; *p < 0.05; **p < 0.01; ***p < 0.001.

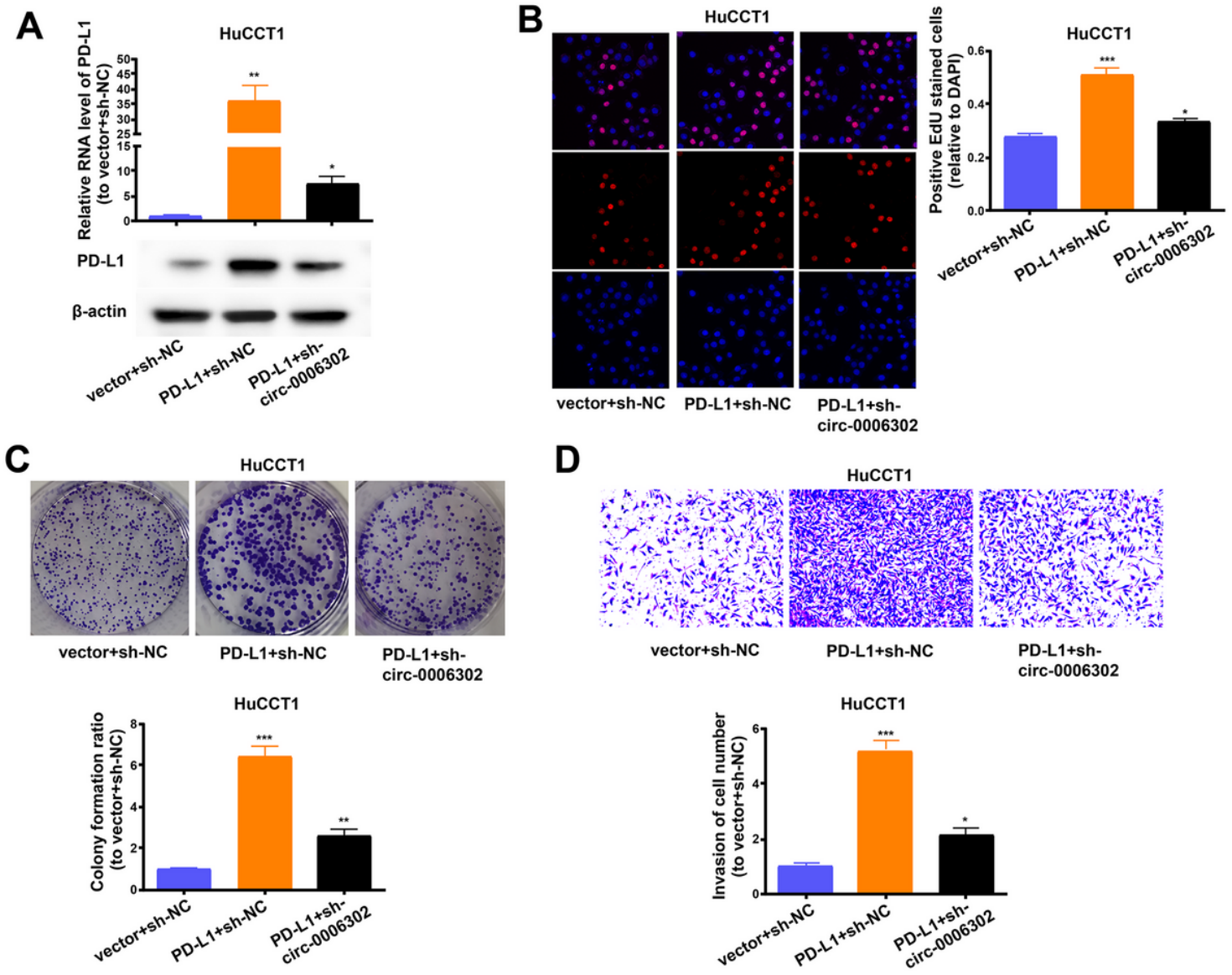

Figure 5

Circ-0006302 knockdown reverses the PD-L1 overexpression-induced increase of proliferation and invasion of CCA cells. (A) Increased PD-L1 expression induced by PD-L1 overexpression is significantly reversed by transfecting circ-0006302 shRNA into CCA cells. (B, C) EdU and colony formation assay show that silencing circ-0006302 significantly reverses the PD-L1 overexpression-induced increase of proliferation and colony forming ability of CCA cells. (D) Silencing circ-0006302 significantly reverses the PD-L1 overexpression-induced increase of invasion in CCA cells. Data represent the mean ± SD of 3 independent experiments; *p < 0.05; **p < 0.01; ***p < 0.001.

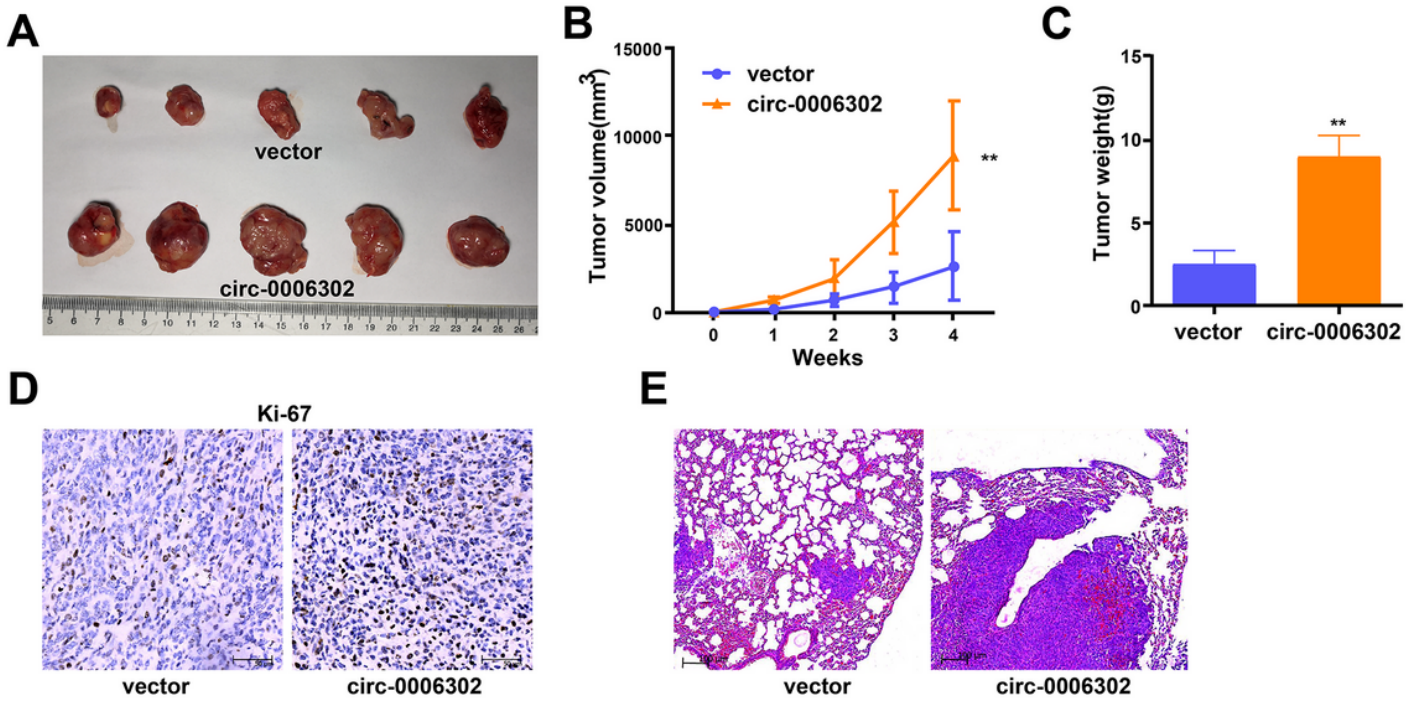

Figure 6

Circ-0006302 promotes the tumor growth and lung metastasis in vivo. (A) Xenograft tumors in a mouse model of CCA. (B) Tumor volumes of the circ-0006302 and vector treatment groups. (C) Tumor weights. (D) Overexpression of circ-0006302 induces the expression of Ki-67 in the xenograft tumors of a mouse model of CCA. (E) Overexpression of circ-0006302 promotes lung metastasis in a mouse model of CCA metastasis. **p < 0.01.

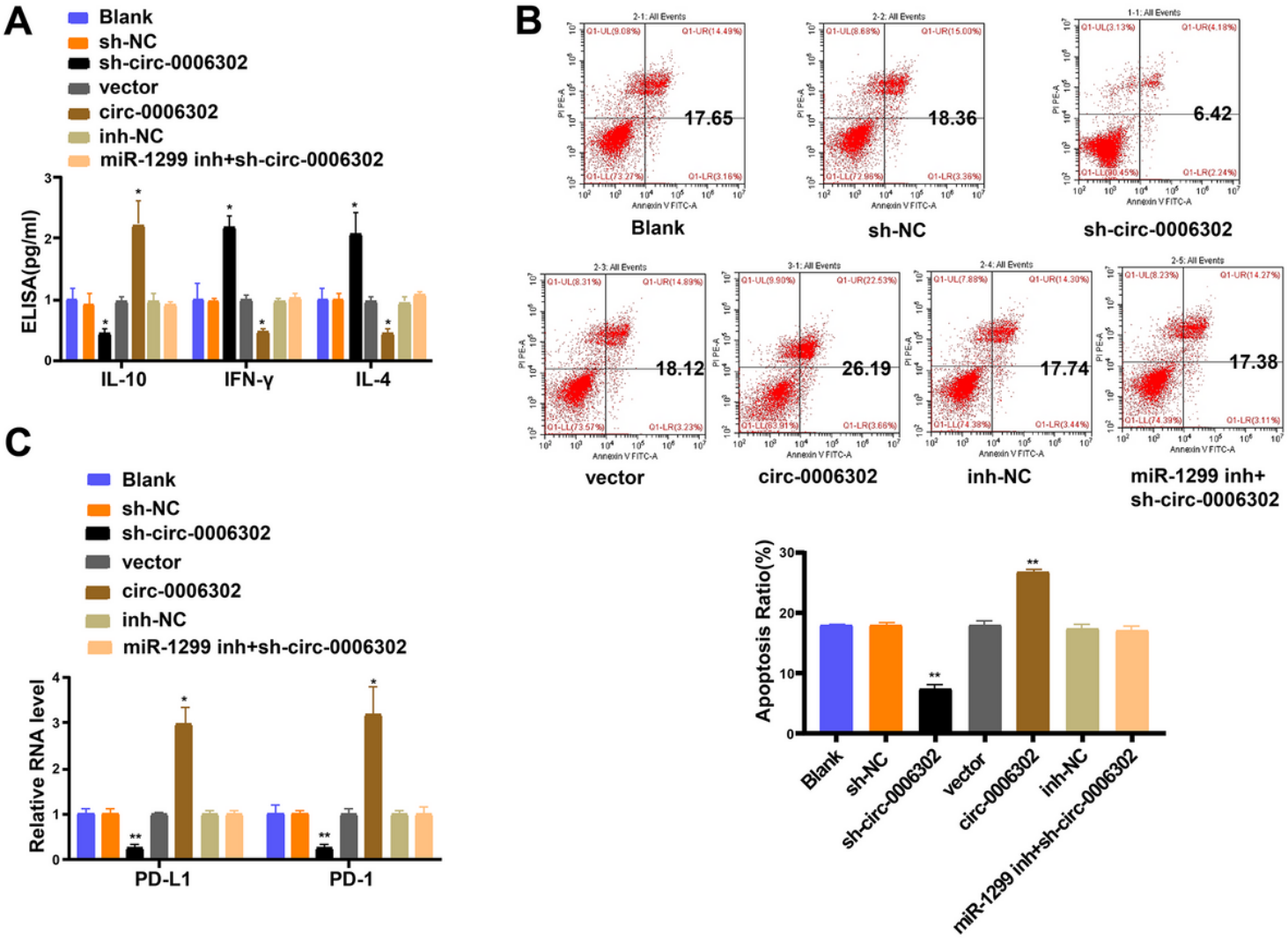

Figure 7

Circ-0006302 sponges miR-1299 to up-regulate the expression of PD-L1 and suppresses the activation of CD8+ T cells. (A) The expression of IL-10, IFN-γ and IL-4 in response to circ-0006302 overexpression or silencing, or inhibition of miR-1299, as detected by ELISA. (B) Cell apoptosis in response to circ-0006302 overexpression or silencing, or inhibition of miR-1299, as assessed by flow cytometry. (C) The expression of PD-L1 and PD-1 in response to circ-0006302 overexpression or silencing, or inhibition of miR-1299, as determined by RT-qPCR. All data were measurement data and expressed as mean ± standard deviation; *p < 0.05; **p < 0.01.

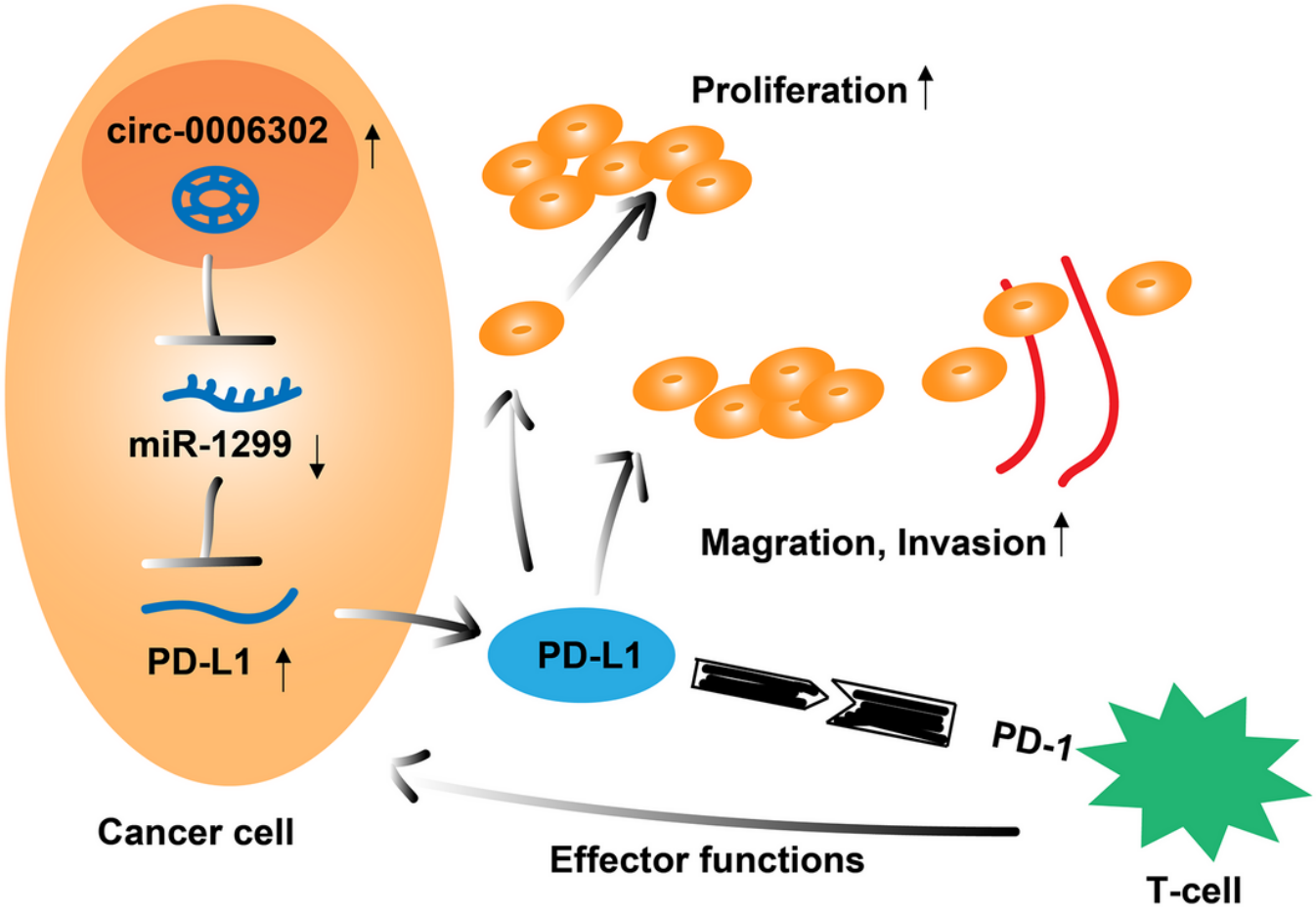

Figure 8

Mechanism diagram underlying the regulatory role that circ-0006302 played in CCA. In CCA cells, circ-0006302 could function as a ceRNA to up-regulate PD-L1, thus inhibiting activation of CD8+ T cells and promoting the progression of CCA.